Sustainable Structures
ISSN: 2789-3111 (Print); ISSN: 2789-312X (Online)
http://www.sustain-dpl.com/journal/sust
DOI: 10.54113/j.sust.2026.000113

ORIGINAL ARTICLE

Innovative hybrid timber floor with simplified construction and calculation fully within the Eurocode 5 to promote sustainable timber-based flooring

Luigi Fenu [a], Angelo Aloisio [b,*], Gian Felice Giaccu [c], Alireza Hosseini [a], Bruno Briseghella [d]

[a] University of Cagliari, via S. Croce n. 59, 09124 Cagliari, Italy
[b] University of L'Aquila, via G. Gronchi n. 18, 67100 L'Aquila, Italy
[c] University of Sassari, Bastioni Marco Polo n. 77, 07041 Alghero (SS), Italy
[d] Fuzhou University, No. 2 Xue Yuan Road, University Town, Fuzhou 350108 - Fujian, China
[*]Corresponding Author: Angelo Aloisio. Email: angelo.aloisio1@ univaq.it

Abstract: Timber–concrete composite floors are currently used as sustainable flooring solutions. To broaden their application, improvements in construction efficiency are required. The hybrid system herein proposed combining timber, steel, and concrete members eases on-site assembly and can be partially prefabricated in factory. Timber beams and steel members, connected with interposed wooden planks through mechanical fasteners, create an oak-beamed ceiling supported by timber–steel composite beams. The steel element, with height equal to the insulating layer already required for energy and comfort purposes, plays a key role during concrete casting, allowing timber-steel composite beams to support fresh concrete and workmen loads with limited deflection. This composite action reduces the timber beam depth, thus lowering material use, and eliminates temporary supports, simplifying construction and reducing costs. These advantages promote wider adoption of timber floors, valued for both sustainability and aesthetics. After concrete hardening, a three-member hybrid floor is obtained. Neither numerical evaluations nor specific experimental tests are required because, even disregarding the steel contribution, the system's performance, simply evaluated with the rules of the Annex B of Eurocode 5, generally accepted also for timber–concrete composites, matches that of conventional solutions with deeper timber beams. The proposed hybrid floor thus combines sustainability, prefabrication, construction efficiency, and compatibility with existing design standards.

Keywords: hybrid timber floors, timber-steel composite beams, self-bearing floor, Eurocode 5 design, sustainable flooring system, prefabrication, thermal insulation

1 Introduction

Nowadays, timber-concrete composite floors are frequently used in new buildings (especially with glued laminated timber beams), as well as in old buildings, where the timber-concrete composite technique is very effective in renovating timber floors, giving them greater stiffness and increasing their load-bearing capacity [1–6]**.** Nevertheless, extension of their applications is needed, and it will be possible through improving structural performances at service and ultimate, as well as through easing their set-in-place during the construction phase. To encourage the adoption of sustainable timber

Received: 24 December 2025; Received in revised form: 4 July 2026; Accepted: 8 July 2026

flooring, this study develops a specific architectural and construction technology. The primary focus is on simplifying construction to overcome a key barrier to its widespread use. Although hybrid timber-based flooring systems have already been investigated in the literature [7–9], the novelty of the present study lies in the proposal of a new hybrid timber floor concept specifically conceived to be self-bearing during the construction phase, thus avoiding temporary propping, while preserving the aesthetic value of the exposed timber soffit and integrating the insulation layer within the total floor thickness. Another distinctive aspect is that, for current applications, the system can be designed through simplified procedures consistent with existing Eurocode 5-based approaches[10], thereby facilitating immediate practical implementation.

Generally, timber-concrete composite (TCC) floors are made of timber beams and concrete slab, the latter cast on wooden planks (that do not perform any structural duty) interposed between the concrete slab and timber beams. Timber beams and concrete slab are mechanically connected by means of steel fasteners, such as nails and dowels. In general, the connection is considered as semi-rigid. This means that timber beams and concrete slab could behave between the two extreme situations of no connection at all (with the two members performing independently and therefore free to slip one on the other) and no slip at all (rigid joint), since slip occurs in any case, but is minimized through appropriate joint systems [2,4,11–14]. Different connection systems have been proposed in the literature for timber–concrete composite floors, including nailed, notched, and inclined-screw solutions [15–29]. In the present paper, these systems are mentioned only to frame the general background of composite floor technology; however, a comparative assessment of their relative mechanical performance is beyond the scope of this study. Since the objective is to present the conceptual design and construction advantages of the proposed hybrid floor, a simplified and practically feasible connection configuration is adopted.

In modern floors an insulating layer is preferable for acoustic and thermal comfort and is usually placed over the concrete slab, thus increasing total floor thickness. This solution is often adopted also in TCC floors (**Fig. 1a**), but another solution is to place the insulating layer over the wooden planks with the concrete slab cast on the insulating layer (**Fig.1b**) and with the vertical sides of the insulating layer used as rib formworks, so that a ribbed slab is obtained.

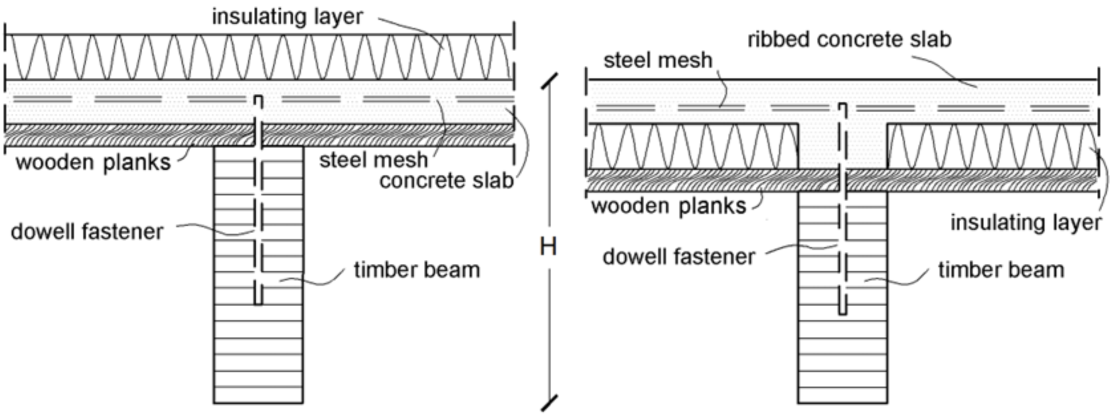

(a) With insulating layer placed over the concrete slab boards (b) With insulating layer interposed between concrete slab and wooden

Fig. 1. TCC floors with same structural depth.

This means that, on the one hand, the insulating layer can be included within the floor thickness without increasing the total depth (**Fig.1b**). On the other hand, for the same structural depth *H* (see **Fig.1**), this arrangement reduces the depth of the timber beam, which in conventional timber–concrete composite floors lead to larger deflections during the construction phase under the weight of fresh concrete and workers, with the consequent need for temporary props. This drawback is overcome in the proposed system by connecting a steel profile to the timber beam, thereby forming a timber–steel composite beam with sufficient stiffness to support construction-stage loads in a self-bearing manner, (**Fig. 2**).

After the timber–steel composite beams have been assembled and positioned in place, the concrete is cast during the construction phase over the timber planking and, after concrete hardening, the hybrid composite floor of **Fig. 3** is finally obtained. Contrary to the solution of **Fig.1a**, by comparing **Fig. 3** with **Fig. 1b**, it is evident that, in both cases, an insulated layer can be included between the wooden planking and the concrete slab for same floor thickness *H*, thus saving space with respect to the traditional solution of **Fig.1a**. Nevertheless, the hybrid solution of **Fig. 3** has a fundamental advantage with respect to the solution of **Fig.1b**, because while the latter needs the use of props during the construction stage, the hybrid solution self-supports the load of fluid concrete and workmen without the aid of any prop. In the hybrid composite floor herein proposed, the insulating layer is placed at both sides of the steel members (**Fig.3**). This configuration, besides providing clear space for the steel profile (essential for maintaining the self-supporting capacity during construction), allows for easy installation of the insulation alongside the steel profile, improving thermal performance for comfort and energy savings, though without increasing the overall floor thickness.

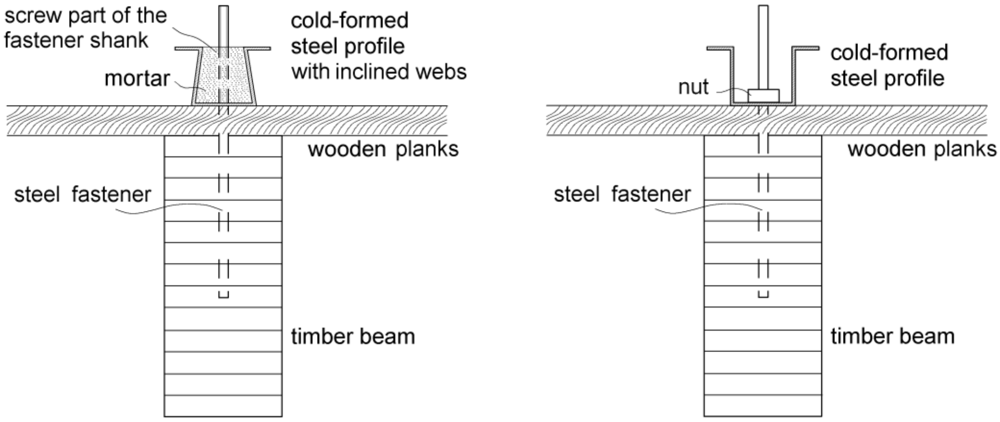

a) By filling channel steel members with mortar b) By locking a nut on the screw part of the fastener sticking out from the top of timber beams.

Fig. 2. Timber-steel composite beams with prevented reciprocal displacement of members

Different sections of omega shaped cold-formed steel members with given depth -but different moments of inertia- are available in the market (**Fig.4**), so that the timber-steel composite beams can be suitably designed to optimize their stiffness in order to bear the load of fluid concrete with very low deflections.

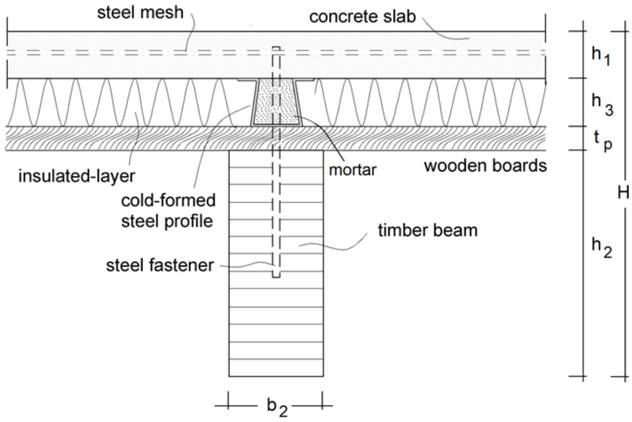

Fig. 3. Hybrid composite floor.

After concrete curing, a hybrid composite floor (HybC) made of three members (timber beam, steel profile and concrete slab) is finally obtained (**Fig.3**). In the scientific literature there are some examples in which the composite technique with timber members and metal profiles is used. Pastori et al. [7] provide a state of the art review of hybrid timber-based structures. Tsalkatidis and Alhussain [8] made a numerical study of a hybrid timber-concrete floor system. Jurkiewiez et al. [30] made an experimental and analytical study of hybrid steel-timber beams in bending. Quang Mai et al. [9] made full scale static and dynamic experiments of hybrid CLT-concrete composite floor. Chybinski and Poulos [31] made experimental and numerical investigations on aluminium-timber composite beams. Gilbert et al. [32]

studied composite timber-steel beams. Zhiyong et al. [33] proposed an innovative Hybrid Timber Floor System (HTFS) which uses post-tensioned concrete beams, cross-laminated timber (CLT) panels, and a concrete topping, all connected with self-tapping steel screws and steel kerf plates. In particular, they demonstrated that timber–steel–concrete floors are particularly suited to meet fire resistance requirements. Owolabi & Loss, Aloisio et al. and Owolabi et al. conducted experimental and numerical studies on the bending and vibration response of hybrid timber-steel composite floors [34–36].

A typical section of the hybrid composite floor considered herein is shown in **Fig. 3**, where the section dimensions and notation are also indicated. This configuration enables the efficient placement of the element adjacent to the steel profile, thereby enhancing thermal performance in terms of both occupant comfort and energy efficiency. Furthermore, this is achieved without increasing the overall floor thickness and while preserving the necessary space for the steel profile to develop composite action with the connected timber beam.

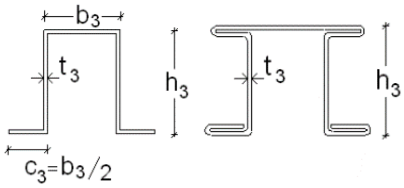

Fig. 4. Omega shaped profiles of the cold-ormed steel members with symmetric felastic section modulus $W_{el.y}$.

The proposed construction and architectural technology can also be effectively applied in the structural upgrading of existing timber floors, particularly in restoration projects, where also a change of use imposing higher load-bearing capacity is required. A common intervention strategy involves casting a reinforced concrete slab over the existing timber planking and ensuring composite action with the underlying wooden beams. However, existing timber beams often lack the capacity to support the wet concrete during casting, thus necessitating temporary propping. The proposed solution addresses this issue by prior connecting a steel profile to the timber beam, thereby increasing its load-bearing capacity and enabling it to sustain the fresh concrete load during the construction phase without additional temporary supports. Note, that while the role of the steel profile is fundamental in the construction phase, after floor completion its contribution to resistance and stiffness of the hybrid composite floor can be even neglected in current applications.

This paper presents the conceptual design of a novel hybrid timber composite floor, developed to simplify construction and encourage wider adoption. Another key advantage of the proposed system is that it can be designed using existing Eurocode 5 rules; in fact, Eurocode 5, in Annex B, provides rules for designing structures composed of two or three timber elements connected to each other by steel fasteners. However, it is generally accepted to extend these rules to both timber-steel and timber–concrete composite structures, (see for instance [4,7]), and therefore to timber–concrete composite floors. The application of these rules to timber–steel composite beams during the construction stage, and their subsequent extension to the hybrid composite floor under the assumptions outlined in Section 4, enables practitioners to design this type of hybrid composite floor without the need for specific physical testing or complex finite element modelling. This allows for immediate implementation based on simple calculations, offering significant benefits in construction speed, ease of assembly, thermal insulation and architectural quality. While future research will investigate the specifics of the system's behaviour, the focus of this work is to establish a viable and practical construction technology that is advantageous in many ways, in particular in sustainability.

The paper is organized as follows. Section 2 describes the hybrid composite floor. Section 3 shows how to assemble timber-steel composite beams and evaluate their static response in the temporary stage of construction. Section 4 shows that, in current applications, the performances of the hybrid composite (HybC) floors herein proposed are sufficiently good in terms of both stress level in floor members at ultimate and deflections at serviceability even disregarding the contribution of the steel profile (instead indispensable in the construction phase), so that calculations can be carried out with the rules of the Eurocode 5 currently used for timber-concrete composite floors. Section 5 compares the structural performances of HybC floors with those of traditional TCC floors with same structural depth. The Conclusions are in Section 6.

2 Hybrid composite floor description

The hybrid composite floor (span L) under consideration is made of timber-steel composite beams with spacing s_p (timber beams with breadth b_2 , depth h_2, and steel members with height h_3) and concrete slab with thickness h_1 cast on the insulating layer (**Figs. 4, 5, 6**). The latter (thickness h_3) and the steel members are placed over wooden planks with thickness t_p, that, to simplify construction, are interposed between steel members and timber beams (**Fig. 5**). Vertical steel dowel fasteners with diameter d are used [2], With the concrete slab cast on the insulating layer, the total structural depth of the hybrid composite floor is hence $H=h_2+ t_p+ h_3+ h_1$. **Figs. 5** and **6** show a render of the timber-steel composite beams and of the hybrid composite floor, respectively.

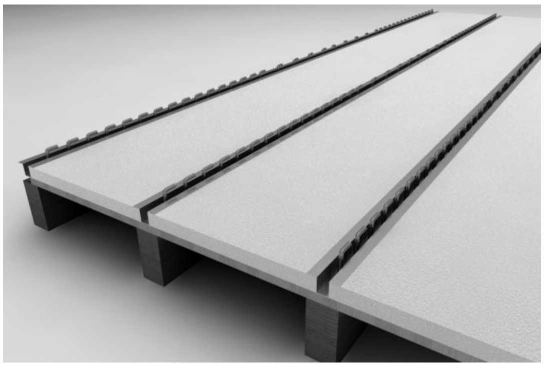

Fig. 5. Render of the timber-steel composite beams with the insulated layer placed aside of the steel profiles and over the wooden plank

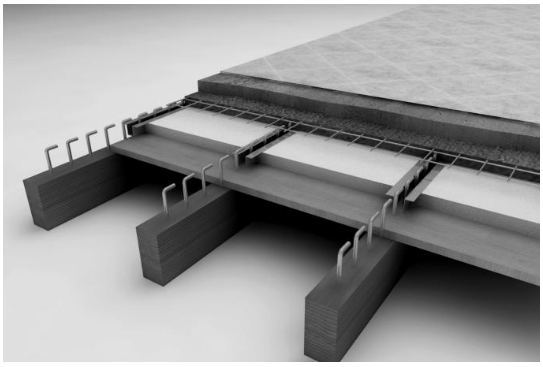

Fig. 6. Render of the hybrid composite floor with timber beams, steel fasteners, wooden plank, steel with a steel mesh, and covered by a tile flooring.

Since conceptualization and sake of simplicity are two of the key features of this paper, only vertical steel dowelled fasteners are herein considered, even if, in general, inclined fasteners are more effective in transmitting the connection force (primarily by axial action), especially when an ineffective layer is interposed between timber beams and deck [15–19]. Nonetheless, they are widely used in the practice thanks to their ease of installation. The vertical dowel fasteners are bent at 90° to provide better anchorage in the concrete (**Figs. 5 and 6**). The presence of the interposed plank increases the flexibility of vertical shear studs, thus increasing slip between the connected members and decreasing the global floor stiffness. According to theoretical studies and experimental results [37, 38] this effect can be accounted for by choosing a suitable value of the slip modulus of the connection [39, 40].

The dowel fastener connection, besides preventing slip between members, prevents the separation in the vertical direction of the steel members from the timber beams during the construction phase. This aim can be achieved by either locking a nut on the screw part of the fasteners sticking out from the top of the timber beams (**Fig.2b**), or filling the channel steel members with mortar, provided that mortar bonding with both fasteners and steel members is assured. For this purpose, fasteners with screw shanks and steel members with inclined webs (**Fig.2a**) or with a pattern of "embossments" into the web surface can be used. In the following, the cross-section of the cold formed steel members is assumed to be sufficiently compact that the effective elastic section modulus $W_{el.y.eff}$ coincides with the elastic section modulus $W_{el.y}$. Moreover, for sake of simplicity and without losing in generality, symmetry of $W_{el.y}$ is supposed.

After assembling the timber-steel composite beams and setting them in place, the concrete slab can be cast without any use of props, scaffolding and formworks because the composite action of timber beams and steel profiles is able to bear the load of fluid concrete and workmen. This feature plays a key role in simplifying the construction of timber floors with high load-bearing capacity, as enabled by an appropriate use of the composite technique. After concrete curing, the hybrid composite floor is finally obtained, with the concrete slab mostly in compression to provide the main contribution to the compression resultant of the floor moment of resistance.

Although the concrete slab reinforced by a steel mesh provides a contribution to the collective two-way field effect of TCC floors, as investigated by some authors [41]**,** this contribution is generally neglected in the practical design of composite floors, because the stiffness in the direction of floor beams is usually much higher than in the transverse direction. This hypothesis is herein adopted, thus considering the composite floor as a one-way floor system made of parallel strips, each one behaving as a beam, thus simplifying the calculations.

2.1 Design values of material strengths and elastic moduli

Strength of timber beams, steel members, and concrete slab depend, respectively, on timber and steel grade, and concrete class. With reference to the Eurocode 5 [10], the design strength of timber members for, respectively, pure tension, pure bending and pure shear is $f_{t.0.d}= k_{mod}\, f_{t.0.k}/\gamma_m$, $f_{m.y.d}= k_{mod}\, f_{m.y..k}/\gamma_m$, $f_{v.d}= k_{mod}\, f_{v.k}/\gamma_m$, where k_{mod} takes account of the effect of the duration of load on strength reduction, and γ_m is the partial safety factor for timber strength. By then referring to the Eurocode 2 [42] and the Eurocode 3 [43], design strength of concrete and yield stress of steel are $f_{cd}=\alpha_{cc}\, f_{ck}/\gamma_c$ and $f_{yd}= f_{yk}/\gamma_{M0}$, respectively, where γ_c and γ_{M0} are the partial safety factors for material strength, and α_{cc} (usually assumed equal to 0.85 in concrete structures, and equal to 1 for short-term loads) takes account of time-dependent effects on concrete strength.

Since deformation of concrete slab and timber beams is time-dependent, deflections at serviceability induced by short-term loads are calculated through their respective elastic moduli E_1 and E_2, while deflections induced by long-term loads are calculated through their related effective values $E_{1.eff}=E_1/(1+\phi)$ and $E_{2.eff}=E_2/(1+k_{def})$, where ϕ is the creep coefficient of concrete, and k_{def} is a creep-mechano-sorpitive coefficient of timber, whose suitable values are available in the scientific literature [10]. In the following, when referring to the effects of short- and long-term loads, the subscripts 0 and ∞ are respectively used. Therefore, $E_{1.0}$ and $E_{2.0}$ indicate the short-term values of the elastic moduli of concrete and timber, respectively, while $E_{1.\infty} = E_{1.eff}$ and $E_{2.\infty} = E_{2.eff}$ indicate their long-term values.

In addition, even the semi-rigid behaviour of the mechanical connection is time dependent, as being related to the elastic moduli of the connected members and depending on creep effects in timber beams and concrete slab.

3 Timber-steel composite beams in the temporary construction phase

Annex B of the Eurocode 5 [10], provides the rules to design timber-composite beams with reference to T and I timber composite beams with the web member respectively connected to an upper flange, and to an upper and a bottom flange made of timber members and/or wood-based panels, see Section B.1.2 of the Annex B. It is generally accepted the extension made by many authors of these rules to timber-steel composite beams and to timber-concrete composite beams (see for instance [4,7]), and herein used in timber-steel composite beams with the timber beam extrados connected to a cold formed steel flexural member (instead of to a concrete slab or a timber top flange), see the following section 3.1.

3.1 Stiffness of timber-steel composite beams

3.1.1 Slip modulus

In this study, the composite technique is first used to obtain timber-steel composite beams with both steel and timber subjected to compression and bending in order to resist loads during the construction phase (C Ph), i.e., the weight of fresh concrete and workers with their equipment. At this phase, deflections of the timber-steel composite beams must be strictly controlled in order to finally obtain a concrete slab with only slightly varying thickness. It is therefore necessary to first evaluate slip modulus at service K_{ser} of the steel-to-timber connection for deflection calculation at the Service Limit State (SLS), that is under the fluid concrete and workmen loading during the C Ph.

For timber-to-timber connection, the Eurocode 5, Section 7.1 [10], suggests to relate K_{ser} to the diameter of the dowel fastener d and the timber density ρ_k , that is:

$$K_{ser} = \rho_k^{1.5} d / 20 \tag{1}$$

For steel-to-timber connections, to take into account the higher rigidity of steel with respect to timber, the same Section 7.1 suggests to double the slip modulus at service state with respect to K_{ser} .

However, Gelfi and Giuriani [44] noted that when strengthening timber beams of wooden floors with a collaborating steel sheet placed over the wooden plank and connected to the timber beams with studs passing through the wooden plank, the interposition of the latter between timber and steel member reduces the connection stiffness. By referring to the Winkler theory of beams on an elastic medium, they obtain the inverse of K_{ser} as:

$$\frac{1}{K_{\mathrm{ser}}}=\left(\frac{t^3}{3EJ}+\frac{t^2}{\mu}+\frac{2\alpha}{k_{\mathrm{w}}}\right)-\frac{\left(\frac{t^2}{3EJ}+\frac{t}{\mu}+\frac{2\alpha^2}{k_{\mathrm{w}}}\right)^2}{\frac{t}{EJ}+\frac{t}{\mu}+\frac{4\alpha^3}{k_{\mathrm{w}}}} \tag{2}$$

with:

$$\alpha=\left(k_{\mathrm{w}}\ /\ EJ\right)^{1/4} \tag{3}$$

where k_w is wood stiffness, J is the inertia moment of the studs, E is the Young modulus of steel, t is the vertical distance between the extrados of the timber beam and the centroid of the steel sheet, and μ is the rotational stiffness of the steel sheet.

Gelfi and Giuriani also validated the results obtained from (2) using experimental tests [44], and pointed out that the influence of μ variations on the value of K_{ser} was very low (e.g. K_{ser} varying less than 5% for doubling μ from 10 to 20 kNm/rad). In this paper K_{ser} estimation of timber-steel composite beams is done through (2).

3.1.2 Flexural stiffness

Flexural and axial stiffnesses of the two members with no connection at all are respectively expressed as

$$EJ_{//}=E_2J_2+E_{3J_3} \qquad EJ_{//}=1/\left[1/\left(E_2A_2\right)+1/\left(E_3A_3\right)\right] \tag{4}$$

where A_2 and J_2 are the cross-sectional area and moment of inertia of the timber beam, and A_3 and J_3 those of the steel profile.

For a composite system with rigid connection, the problem can be faced in terms of differential equations [45], whose solution can be obtained in close form for simply supported beams with uniformly distributed load and/or a concentrated load at mid-span..

In case of semi-rigid connections, the approach of the Annex B of the Eurocode 5, with introduction of connection efficiency factors, can be followed. In fact, it allows to extend the case of T composite beams made of two timber members to the case of timber-concrete and timber-steel composite beams [10,46].

After introduction of connection efficiency factors γ_i (in this case i=2,3 for timber and steel, respectively), the effective flexural stiffness of the composite beam can be defined as:

$$\left(EJ\right)_{\mathrm{ef}}=\left(EJ\right)_{//}+\gamma_2E_2A_2a_2^2+\gamma_3E_3A_3a_3^2 \tag{5}$$

where a_2 and a_3 are, respectively, the distances of the centroids of timber and steel members from the system centroid $G_{2.3}$ (**Fig. 7**). The position of the latter with respect to the lower edge of the timber beam is:

$$y_{\mathrm{G}_{2\text{-}3}}=\frac{\gamma_3E_3A_3\left(t_{\mathrm{p}}+h_2+\frac{h_3}{2}\right)+\gamma_2E_2A_2\frac{h_2}{2}}{\gamma_3E_3A_3+\gamma_2E_2A_2} \tag{6}$$

while a_2 and a_3 are expressed as:

$$a_2 = \frac{\gamma_3 E_3 A_3 \left(t_\mathrm{p} + \frac{h_2}{2} + \frac{h_3}{2} \right)}{\gamma_3 E_3 A_3 + \gamma_2 E_2 A_2} \qquad a_3 = \left(t_\mathrm{p} + \frac{h_2}{2} + \frac{h_3}{2} \right) - a_2 \tag{7}$$

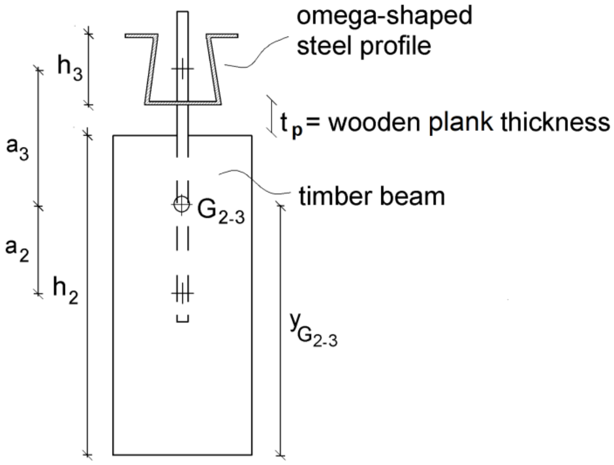

Fig. 7. Geometry of the timber-steel composite beam

The connection efficiency factors take into account the efficiency of the connection, assuming the value zero for no connection at all and 1 for a perfect-rigid connection. Assumed $\gamma_2 = 1$, the expression of γ_3 is:

$$\gamma_3 = \frac{1}{1 + \frac{\pi^2 E_3 A_3 s_\mathrm{eq}}{K l^2}} \tag{8}$$

where K is the slip modulus, coinciding with K_ser at S.L.S., and with $s_\mathrm{eq} = 0.75\ s_\mathrm{min} + 0.25\ s_\mathrm{max}$ for fasteners whose spacing varies along the beam [3]; where s_eq is the effective spacing of the fasteners, s_max and s_min are their maximum and minimum spacing, respectively.

3.1.3 Subdivision of the internal forces proportionally to members' stiffness

The internal forces can be calculated as in timber-to-timber or in timber-concrete composite beams. Timber and steel members are subjected to combined normal force and moment. According to the Annex B of the Eurocode 5 [10], these internal actions can be respectively expressed as:

$$N_\mathrm{i} = \frac{\gamma_\mathrm{i} E_i a_\mathrm{i} A_\mathrm{i}}{(EJ)_\mathrm{ef}} M \qquad M_\mathrm{i} = \frac{E_\mathrm{i} J_\mathrm{i}}{(EJ)_\mathrm{ef}} M \tag{9}$$

where, in evaluating $(EJ)_\mathrm{ef}$ and γ_3 in (9), the ultimate and service values K_u and K_ser of slip modulus K are respectively used for checking timber and steel members at U.L.S. and S.L.S..

Since the timber-steel composite beams under consideration work in the short term, then the time dependency of the timber beams is neglected. Only short-term checks at both ultimate and service limit states are therefore required.

3.2 Ultimate Limit State

Following the Annex B of the Eurocode 5 [10], at ultimate the design moments M_d are considered, thus allowing to calculate the normal stresses

$$\sigma_\mathrm{i} = \frac{\gamma_\mathrm{I} E_\mathrm{i} a_\mathrm{i}}{(EJ)_\mathrm{ef}} M_\mathrm{d} \qquad \sigma_\mathrm{m.i} = \frac{0.5 E_\mathrm{i} h_\mathrm{i}}{(EJ)_\mathrm{ef}} M_\mathrm{d} \tag{10}$$

which are respectively due to axial force and bending moment, with i=2, 3 for timber and steel, respectively, and with $(EJ)_\mathrm{ef}$ evaluated in the short-term, that is with the short-term values of E_2 and K_u.

Therefore, checking timber beams subjected to combined tensile force and moment at the U. L. S. requires that $\sigma^{\prime(2)} \leq 1$, where

$$\sigma^{\prime(2)} = \left(\sigma_2 / f_{\mathrm{t.0.d}} + \sigma_{\mathrm{m.2}} / f_{\mathrm{m.y.d}}\right) \tag{11}$$

while checking steel members (instead subjected to combined compressive force and moment) the maximum compressive stress at the short-term in steel members is $\sigma^{(3)} = |\sigma_3 + \sigma_{\mathrm{m.3}}|$, the latter still evaluated with the short-term value of $(EJ)_{\mathrm{ef}}$. Since shear stresses in the webs are always very low, with therefore negligible effects on Von Mises stress level, section resistance is hence adequate if $\sigma^{\prime(3)} = \sigma^{(3)} / f_{\mathrm{yk}} / \gamma_{\mathrm{M0}} \leq 1$,where, according to the Eurocode 3 [47], γ_{M0} is the partial factor for cross-section resistance.

Shear force on the dowel-type fastener with diameter d depends on shear V_{d}, and is expressed as

$$F_{\mathrm{3.d}} = \left(\gamma_3 E_3 a_3 s_{\mathrm{eq}} / (EJ)_{\mathrm{ef}}\right) V_{\mathrm{d}} \tag{12}$$

It cannot exceed the bearing resistance of the steel member as prescribed in the Eurocode 3 [47]

$$F_{\mathrm{b.Rd}} = k_1 \alpha_{\mathrm{b}} d t_3 f_{\mathrm{uk}} / \gamma_{\mathrm{M2}} \tag{13}$$

where α_{b} and k_1 control, respectively, plate tear-out by shearing in the direction of load transfer and plate tension fracture perpendicular to the direction of load transfer, and where γ_{M2} is the partial factor for connection resistance.

However, while the U.L.S. is not critical for this kind of timber-steel composite beams, as shown in the next Section 3.4, the magnitude of deflections at the S.L.S. in the construction stage is instead critical, as explained in the next Section 3.3.

3.3 Service Limit State

At the Serviceability Limit State (SLS), deflections of timber-steel composite beams during C Ph -when temporary loaded by fresh (non-hardened) concrete and construction live loads, i.e. workers with their equipment- must be adequately controlled. In fact, excessive deflections at this stage may result in an unintended curvature of the concrete slab intrados, thus potentially increasing the slab's self-weight excessively, and may also lead to visually unacceptable deformations of the exposed timber elements. Both timber and steel members must be sized to limit these deflections. For this aim, it can be noted that, for given depth, stiffness of cold-formed steel members can be easily increased by increasing core thickness, or by choosing cold-formed profiles, whose peculiar shape significantly increases both moment of inertia and cross-sectional area (see **Fig. 4**). It should be noted that timber-steel composite beams could become even stiffer than timber beams with the same depth.

$$u_{\mathrm{p}} = \chi \frac{5}{384} \frac{p_{\mathrm{k}} l^4}{(EJ)_{\mathrm{ef}}} \qquad u_{\mathrm{Q}} = \chi \frac{1}{48} \frac{Q_{\mathrm{k}} l^3}{(EJ)_{\mathrm{ef}}} \tag{14}$$

At S.L.S, after substitution in (8) of K with K_{ser} as expressed in (2), and after updating $(EJ)_{\mathrm{ef}}$, the displacement u at mid-span, induced by the uniformly distributed load p_{k} of the fluid concrete and by the workmen live load (concentrated load Q_{k}), is the sum of u_{p} and u_{Q}: with u_{p} and u_{Q} respectively expressed as: where χ is a coefficient accounting for shear deformations.

3.4 Performance of timber-steel composite beams during the construction phase.

To construct HybC floors with the technology described in the previous sections, specific performance of the timber-steel composite beams in terms of deflections at serviceability during the C Ph are required. The ultimate strength of the timber–steel composite beams is also taken into account; however, since they are sized to meet the stringent serviceability requirements of the C Ph necessary to maintain a sufficiently uniform concrete slab thickness, their strength during the C Ph is more than adequate.

3.4.1 Service performance of timber-steel composite beams in terms of deflections

Consider timber-steel composite beams made of timber beams with beam depth h_2 = 230, 240, 250 mm and given width b_2=100 mm, as well as with omega-shaped steel profiles with h_3=50, 60 mm (b_3=40 mm, c_3=20 mm, t_3=2 mm). The timber beams are spaced s_p=667 mm, and the fastener's effective spacing s_e is 125 mm The gap between timber beam and steel profile is 22 mm, coinciding with the wooden plank thickness t_p (See **Fig. 7**). After floor completion, the slab thickness of the hybrid composite floor will be h_1=50 mm. Floor span lengths L of 5, 6 and 7 m are considered.

For L= 5 m, h_2=240 mm and h_3=50 mm (corresponding to a hybrid composite floor with total thickness H= $h_2 + h_3 + h_1 + t_p$ = 362 mm), deflection of timber-steel composite beams induced by workmen and fluid concrete during the construction phase (C_Ph) is 4.5 mm, that is a quite small deflection value that allows to prevent the use of props. Moreover, for same span length L = 5 m and h_1=50 mm but lower floor structural depth H = 352 mm, that is h_2=230 mm and h_3=50 mm, the deflection of the timber-steel composite beam under floor construction is increased to only 4.9 mm. Such small deflections lead to so small an increase of the load due to fluid concrete that, during the C Ph, would result in a deflection increase of only 0.15 mm of the timber-steel composite beams. After floor completion, the effects of this small an increase of concrete volume is negligible for the performances of the hybrid composite floor.

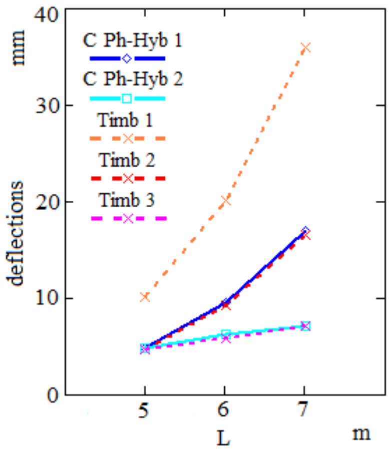

Fig. 8. Deflections of timber-steel composite beams during C Ph for given h_2 and varying L, and comparison with the deflections of timber beams of TCC floors during their construction phase.

Fig. 8 shows that, if the span length varies (L=5-7 m) and the depths of the timber beam and the steel profile are given (i.e. h_2 = 230 mm and h_3 = 50 mm (see C_Ph-Hyb 1 in **Fig. 8**), deflections of the timber-steel composite beams increases significantly for increasing span length, meaning that, for same steel profile, by increasing span length the timber beam depth should be increased, too. Note that, for same L = 5, 6 and 7 m, in traditional TCC floors with same timber beams' depth h_2=230 mm, the displacement at mid-span of the timber beam only (see Timb 1 in **Fig. 8**) caused by fluid concrete and workmen during concrete cast would increase dramatically.

The use of props would become therefore necessary, with cost increase for scaffolding. This drawback could be overcome only through increasing h_2. For instance, for h_2 = 280 mm, the deflections during the construction phase of Timb 2 in **Fig. 8** are practically the same as the ones of the timber-steel composite beam C_Ph-Hyb 1.

Unfortunately, h_2 = 280 mm is an excessive timber beam depth for a timber-concrete composite floor when, after floor completion, the composite action with the concrete slab would be wholly developed and such an oversized timber section would become unexploited. **Fig. 8** also shows that, if deflections under the construction phase are limited to L/1000 (as it nearly happens for C Ph-Hyb 1 deflecting only 4.9 mm for L = 5 m), than the depths of timber beam and steel profile must be suitably chosen to obtain the small deflections of the curve C Ph-Hyb 2 in **Fig. 8**. For instance, for same slab thickness h_1 = 50 mm, one can obtain deflections of 4.9 mm for L = 5 m, 6.3 mm for L = 6 m and 7.1 mm for L = 7 m, corresponding to timber beams with h_2 = 230, 270, 330 mm respectively connected to steel profiles with h_3 = 50, 60, 60 mm (see curve C Ph-Hyb 2 in **Fig.8**). No standard explicitly prescribes a deflection limit of L/1000 for the construction stage in the present case. This value has been adopted herein as a practical and conservative criterion to ensure that the increase in slab thickness caused by beam deflection remains negligible and that the final geometry of the slab complies with the tolerances required during execution.

In traditional TCC floors similar deflections under the loads of fluid concrete and workmen would be achieved with h_2 = 300, 350, 400 mm for L = 5, 6, 7 m, respectively (see Timb 3 in **Fig. 8**), that are indeed high values of h_2 for TCC floors after their completion.

Note that only steel profiles with h_3 = 50-60 mm have been herein considered, that is with thickness 50-60 mm of the insulated layer, that are values currently used to achieve a good comfort level. If higher values of h_3 were considered, deflections of the timber-steel composite beams could have been even lower.

3.4.2 Stress level at ultimate of timber-steel composite beams under factored loads

While the sizing of timber-steel composite beams is highly affected by deflection limits during the C Ph, it is not affected by stress level at ultimate evaluated in accordance to the Eurocodes 3 and 5 [10,43]. Tab. 1 shows stress level in timber and steel members during the C Ph for given timber beams' depth h_2=230 mm and varying L, as well as for given L= 5 m and varying h_2. In both cases, checking the timber beams subjected to the loads of fluid concrete and workmen at the U.L.S., stress level is largely within the limits of timber strength according to the Eurocode 5 prescriptions.

Table 1. Stress level in timber and steel members during the C Ph

For given L=5 m	h_2=230 mm	h_2=240 mm	h_2=250 mm
$\sigma'^{(2)}$	0.273	0.257	0.242
$\sigma'^{(3)}$	0.317	0.296	0.277
For given h2=230 mm	L = 5 m	L = 6 m	L = 7 m
$\sigma'^{(2)}$	0.273	0.362	0.463
$\sigma'^{(3)}$	0.317	0.443	0.588

Finally, for the steel omega shaped profile described at the beginning of this section and for steel dowel fasteners with d=14 mm, f_y = 800 MPa, and equivalent spacing s_e =125 mm, calculations show that, for h_2=230 mm and L=5 m, during the C Ph the shear strength of the fastener, as well as the bearing strength of the steel profile, are much higher than the shear force on the fastener. In fact, it is however lower than that in the hybrid composite floor, where the contribution of the slab is added.

4 Hybrid composite floors

This article presents a hybrid timber-steel-concrete composite floor designed to simplify construction and reduce costs. Ultimately, the system promotes the wider adoption of sustainable timber construction by combining simple, code-compliant calculations with practical construction techniques that maintain the high architectural quality of timber ceilings.

The incorporation of a steel profile provides sufficient stiffness during the construction phase to support the wet concrete and construction loads without temporary propping [48]. This offers a significant advantage over conventional TCC systems, leading to lower labor costs, potential for partial prefabrication, and a streamlined on-site process. Notably, the structural role of the steel member is primarily essential during construction, while in most practical applications, its contribution to the completed floor's performance can be neglected for design purposes.

This is a key assumption that, by using analytical methods, analogous to those already employed for timber–steel composites in Section 3, allows designers to extend to this case the design rules of Annex B of Eurocode 5, currently applied to timber–concrete composite floors, as outlined in Section 3. In fact, as established for three-layer composite systems, damage to the intermediate layer results in a reduction in structural efficiency, affecting both strength and stiffness [49]. By analogy, in the present case, the intermediate member (i.e., the steel profile) is assumed to be ineffective, such that the overall load-bearing capacity and stiffness are governed exclusively by the residual composite interaction between the timber beams and the concrete slab. The omission of the enhanced performance that the steel profile could provide is offset by the simplification of the calculations and by the possibility of relying on design procedures based on existing standards. This means that calculations at S.L.S. and U.L.S. can be easily made by only considering axial force and moment in the timber beam and in the concrete slab. Therefore, all formulae from (4) to (12) describing the composite action of the timber beam prevalently in tension connected to another member (in this case, the concrete slab prevalently in compression) remain valid, with the only difference that the subscript 1 referred to the concrete slab replaces the subscript 3 referred to the steel profile.

In fact, if we consider a HybC floor with same structural depth of a TCC floor (the former with timber beam depth such that, added to the depth of the steel profile, is equal to the timber beam depth of the latter), the results show that the performances of the hybrid composite floor in terms of both stress and deformations at S.L.S. and U.L.S. are within the limits of the reference Code (i.e. the Eurocode 5) while neglecting the contribution of the steel member.

Moreover, they are well comparable to those of the TCC floor with same structural depth. The issue solved by the proposed HybC floor and the consequent advantages in the construction procedure are exactly highlighted by this comparison. In fact, on the one hand a TCC floor with same structural depth of the HybC floor would have an excessive timber section, only necessary to avoid the use of props and scaffolding. On the other hand, the HybC floor allows to reduce the depth of the timber beams without entailing further costs for props and scaffolding.

Note that, by neglecting the contribution of the steel profile, for calculation purposes the HybC floor can be brought back to be considered as a timber-concrete composite floor, with calculations based on the Eurocode 5. This approximation leads to conservative performances, that in the following will show to be practically equivalent to those of TCC floor with same structural depth (that is same distance between the concrete slab extrados and the timber beam intrados), but with higher timber beam depth.

The neglected contribution of the steel profile to the performances of the hybrid composite floor will be the subject of future research, Of course, the higher the moment of inertia and cross-sectional area of the steel profile, the higher will be its contribution. It will also benefit from the higher slip modulus provided by the dowel fastener connection, the higher the thicker the steel profile flange, that is passed through by the dowel fastener, thus providing higher bearing force to the fastener shaft above the wooden plank gap, as described in the next section 4.1.

4.1 Stiffness of hybrid composite floors

Once concrete is cured, the stiffness of the hybrid composite floor is mainly due to the composite action of timber beams and concrete slab. The steel profile contribution is hence conservatively disregarded in calculating floor deformation. With the calculation simplification allowed by the use of the formulations of the Annex B of the Eurocode 5 on composite timber beams, stiffness can be readily available with no specific numerical and/or experimental investigations.

Similarly to the previous case of timber-steel composite beams, the connection stiffness is affected by the interposition of the wooden plank. Gelfi et al [37,38] suggested that, in timber-concrete composite beams, slip modulus can be analytically obtained provided that the embedment of the steel dowel fastener is higher than 6*d* in the timber beam and 3*d* in the concrete slab, as it usually happens in practice. Since cement mortar is placed between the two inclined webs of the omega-shaped profile to prevent vertical displacement relative to the timber beam, Gelfi's method for evaluating the slip modulus of timber-concrete composite floors with an interposed wooden plank is adopted.

In the absence of experimental results, by modelling the steel dowel fastener as a beam in a Winkler medium, the slip modulus K can be assumed as:

$$K = 12\left(\alpha_{c}\alpha_{w}\right)^{3} E_{s}J_{p} / Z \tag{15}$$

with

$$\alpha_{c} = \sqrt[4]{k_{c} / \left(4E_{s}J_{p}\right)} \qquad \alpha_{w} = \sqrt[4]{k_{w} / \left(4E_{s}J_{p}\right)} \tag{16}$$

$$Z = 3\left(\alpha_c^2 + \alpha_w^2\right)\left(\alpha_c + \alpha_w\right) + 3t\alpha_c\alpha_w\left(\alpha_c + \alpha_w\right)^2 + 3t^2\alpha_c^2\alpha_w^2\left(\alpha_c + \alpha_w\right) + t^3\alpha_c^3\alpha_w^3 \tag{17}$$

where: k_c is concrete stiffness, k_w is timber stiffness, E_s, d and J_p are, respectively, elastic modulus, diameter and moment of inertia of the steel dowel fastener, t is the wooden plank thickness.

In the absence of a specific validated slip-modulus formulation for the proposed timber–steel–concrete configuration, it is conservatively assumed that $K_{ser}= K$ as obtained from **(**15**),** that is a formulation valid for conventional timber–concrete composite systems with interposed wooden planking**.** This assumption is conservative, since it neglects the increase in connection stiffness and hole-bearing resistance associated with the presence of the steel profile, through which the dowel fastener passes before anchorage in the concrete. Moreover, the omega-shaped profile together with the concrete (or good quality mortar in case of partial prefabrication) encased between its two webs reduce end rotation of the fastener. This connection system is therefore more effective than that provided by the concrete only, as it currently happens in TCC. The actual slip modulus of the hybrid system is hence expected to be higher than the value assumed herein, as it also results by an initial test campaign aimed to evaluate this effect [50].

In studying any composite structure with timber and concrete members, it must be taken into account that both timber and concrete are affected by creep, so that the behaviour of hybrid composite beams is time-dependent [51,52]. For instance, slip modulus K is time-dependent. Saying $K = K_0$ at time t=0, its expression at time t=∞ is assumed to be $K_\infty=K_0/(1+\psi_2\ k_{def})$, where k_{def} is the so-called mechano-sorpitive coefficient of timber. In general, elastic moduli E_1 and E_2 of timber and concrete depend on the duration of load, and their long-term values $E_{1.\infty}$ and $E_{2.\infty}$ respectively depend on the creep coefficient ϕ for concrete and on k_{def} for timber.

Therefore, flexural and axial stiffnesses depend on the duration of load through E_1 and E_2. Since the steel profile contribution is neglected, they are respectively expressed as in (4), provided that the subscript 1 in place of 3 is put, where 1 is related to the concrete slab.

By then referring to a semi-rigid connection, the effective flexural stiffness $(EJ)_{ef}$ is calculated as in (5) after still substituting the subscript 3 with 1. Equation (5) shows that $(EJ)_{ef}$ depends on the duration of load not only through the elastic moduli E_1 and E_2 of timber and concrete, but also through γ_1, a_1 and a_2.

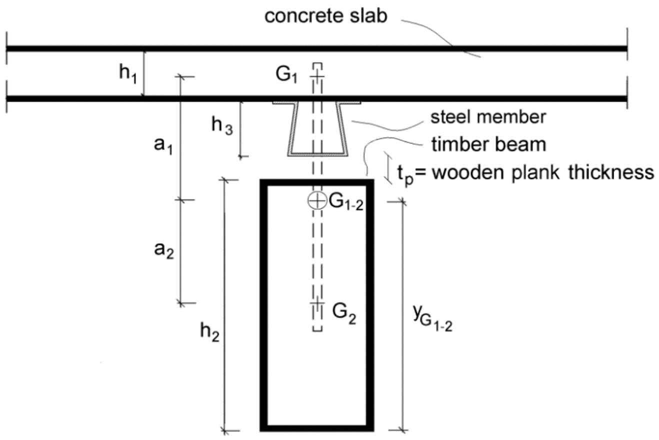

(a) Consequent geometry (in bold) and baricenter identification connection

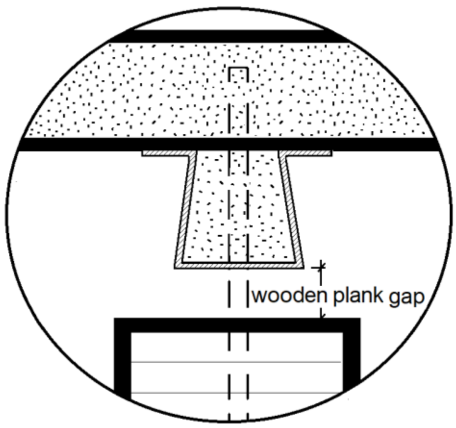

b) Detailed view of the fastener

Fig. 9. Hybrid composite floor with disregarding the steel member contribution

In fact, calculating the centroid position of the composite system (**Fig. 9**):

$$y_{G_{1\text{-}2}} = \frac{\gamma_1 E_1 A_1\left(t_p + h_2 + h_3 + \dfrac{h_1}{2}\right) + \gamma_2 E_2 A_2 \dfrac{h_2}{2}}{\gamma_1 E_1 A_1 + \gamma_2 E_2 A_2} \tag{18}$$

the distances between the centroid G of the composite beam and the centroids of timber and concrete member are then (**Fig. 9**):

$$a_1 = \frac{h_1}{2} + h_2 + h_3 + t_a - y_G \qquad\qquad a_2 = y_G - \frac{h_2}{2} \tag{19}$$

where h_3 is the distance between the concrete slab intrados and the wooden plank extrados (coinciding with the depth of the steel profile) and where a_1 and a_2 depend on the duration of load through y_G, that is, for (10), through E_1, E_2 and γ_1.

4.2 Ultimate Limit State

As discussed in the previous Section 2, the hybrid composite floor under consideration is considered as a one-way floor made of parallel strips that, therefore, are herein considered as hybrid composite beams made of timber and steel members, and concrete slab.

Since the contribution of the steel member is disregarded, only axial force and bending of concrete and timber members are considered. (**Fig. 10**). This leads to conservative ultimate stress values for timber beams and concrete slab, that can be evaluated following the rules of the Annex B of the Eurocode 5 without any specific numerical and/or experimental investigation. **Fig. 10** also shows the favourable effect of the lever arm increase given by the interposed steel profile.

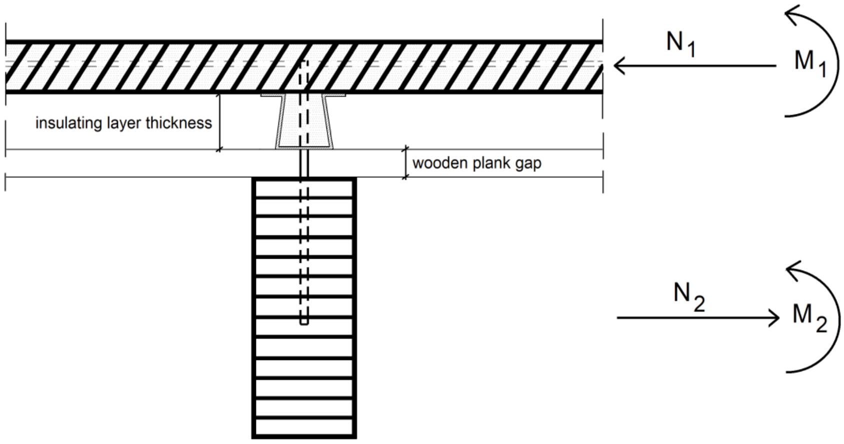

Fig. 10. Simplified calculation model of the hybrid composite floor disregarding the steel profile contribution.

Therefore, having defined K_{ser} as explained in the previous section 4.1, assumed slip modulus at ultimate as $K_u = 2/3K_{ser}$, and calculated $(EJ)_{ef}$, γ_1, a_1 and a_2 , the normal forces N_i and moments M_i in concrete and timber member (i=1,2) are expressed as in Eq. (9), and referred to the design moments M_d.

Since both the flexural stiffness of HybC floor and the strength of timber and concrete depend on the duration of load [53,54], the adequacy of members must be checked for both short- and long-term loads, namely for t=0 and t=∞. Assumed $K_{u.0} = K_u$ in the short-term, for long-term loads, i.e. t=∞, the long-term value at ultimate of slip modulus is $K_\infty = K_0/(1+ \psi_2\, k_{def})$. Also, the long-term values of elastic moduli $E_{1.\infty}=E_{1.0}/(1+\psi_2\, \phi)$ and $E_{2.\infty}=E_{2.0}/(1+\psi_2\, k_{def})$ are likewise defined. Note that in the section 2.3.2, the Eurocode 5 specifies to put ψ_2 =1 in K_∞,, $E_{1.\infty}$, $E_{2.\infty}$ [10] when evaluating the long-term effects of permanent loads at ultimate.

Similarly to the previous section, timber beams (identified by index i=2) have been checked through (11) and (10). Resistance of timber beams under both short- and long-term loads is then adequate if $\sigma_0^{I\,(2)} \leq 1$ and $\sigma_\infty^{I\,(2)} \leq 1$, respectively. For Eqs.(5), (7), (8), (9), $\sigma_\infty^{I\,(2)}$ depends on the duration of load through σ_2 and $\sigma_{m.2}$, as well as through the k_{mod} value applied to timber strength for long-term loading.

Normal stresses σ_1 and $\sigma_{m.1}$ in concrete have been calculated through the expressions (10), upon substitution in (10) of index 2 with 1.

The concrete slab is subjected to axial force in combination with moment; therefore, compressive and tensile stresses at its top and bottom edge, respectively, are expressed as $\sigma^{(1c)}=|\sigma_1 + \sigma_{m.1}|$ and

$\sigma^{(1t)}=|\sigma_1-\sigma_{m.1}|$, thus depending on t through γ_1, E_1, a_1, $(EJ)_{ef}$. Hence, $\sigma_0^{(1c)}$, $\sigma_\infty^{(1c)}$ and $\sigma_0^{(1t)}$, $\sigma_\infty^{(1t)}$ cannot exceed f_{cd} and f_{ctd}, respectively.

The load F on the fastener in a floor region with fastener spacing s and shear force V is calculated as:

$$F=\frac{\gamma_2 E_2 A_2 a_2}{(EJ)_{ef}} \tag{20}$$

Considering failure modes with single shear and fixed dowel support, the load-carrying capacity R per fastener of timber joints is the lowest among the R values obtained, from Johansen's equations [55], and its design value R_d must exceed F_d at both t=0 and t=∞. Even if $(EJ)_{ef}$, E_1, a_2 depend on t, F only slightly changes with time, as shown in the next Section 5.4.

4.3 Service Limit State

Finally, at serviceability, a slip modulus value accounting for the slip increase caused by the interposed plank is assumed.

Say $K_{ser}=K$, as defined in (5). For short-term loads, $K_0=K_{ser}$ is put and, after substituting K with K_0 in (8), the connection efficiency factor γ_1 of concrete for t=0 is then calculated by substituting the subscript 3 with 1 in (8), thus also allowing to update a_1, a_2 as expressed in (19). Consequently, given γ_1, γ_2, a_1, a_2, at time t=0 $(EJ)_{ef.0}$ is then achieved similarly to (5), thus allowing to calculate the short-term deflection $u_0=u_{g.0}+u_{q.0}$, where $u_{g.0}$ (contribution of permanent loads) and $u_{q.0}$ (contribution of imposed loads) are expressed as:

$$u_{g.0}=\chi\frac{5}{384}\frac{g_k l^4}{(EJ)_{ef.0}} \qquad u_{q.0}=\chi\frac{5}{384}\frac{g_k l^4}{(EJ)_{ef.0}} \tag{21}$$

For long-term loads, and therefore t=∞, effective values of slip modulus $K_\infty=K_0/(1+k_{def})$, and of elastic moduli $E_{1.\infty}=E_{1.0}/(1+\phi)$ and $E_{2.\infty}=E_{2.0}/(1+k_{def})$ are then calculated so that the values of γ_1, γ_2, a_1, a_2, at time t=∞ can be obtained. Similarly to (5), the long-term value $(EJ)_{ef.\infty}$ of the effective flexural stiffness is therefore calculated, so that the long-term deflection of the composite floor can be finally obtained as $u_\infty=u_{g.\infty}+\psi_2\, u_{q.\infty}$, where ψ_2 is the load combination factor, and $u_{g.\infty}$ and $u_{q.\infty}$ are calculated by means of (21) after substituting $(EJ)_{ef.0}$ with $(EJ)_{ef.\infty}$. Disregarding the contribution of the steel profile leads to higher compliance of the hybrid floor, but the related displacements have shown to be lower than the Code limits in current applications.

5. Performance comparison with conventional timber-concrete composite floors. results and discussion

This section compares the structural performance of the proposed hybrid timber floor with a conventional Timber-Concrete Composite (TCC) floor of identical thickness, span, and loading. For this analysis, the contribution of the steel profile, essential during construction, is disregarded. This simplification allows the design to be conducted using the established rules of Eurocode 5 for timber composite structures.

Under this assumption, the design requires only the floor geometry and the mechanical properties of the concrete, timber, and fasteners. As demonstrated in the previous section, these readily available inputs are sufficient to verify the floor's performance at both the Ultimate and Serviceability Limit States (ULS and SLS). Consequently, this streamlined design process offers significant advantages to practitioners, facilitating the broader adoption of timber floors as an ecological and sustainable building solution.

The performance improvement afforded by the steel profile is a function of its cross-sectional area, moment of inertia, and material properties. Although accounting for the contribution of the steel profile could further enhance the already good performance of the hybrid composite floor, the following analysis shows that, even when its effects are neglected, the HybC floor under consideration remains sufficiently performant. However, because the steel profile acts in parallel with the concrete slab relative to the timber beam, its contribution falls outside the scope of current Eurocode 5 provisions for timber composite structures. Furthermore, as the dowel fastener engages both the concrete slab and the steel profile in series, quantifying this contribution would require either an experimental determination of the slip modulus for this specific configuration or the development of a sophisticated numerical model. A significant challenge would be generalizing such results for different steel profiles, a problem that lies beyond the scope of current design practice and warrants dedicated future research.

Therefore, this paper focuses on the conceptual design of this hybrid floor system, emphasizing the immediate advantages it offers: simplified construction and a design methodology based on existing standards. By demonstrating a viable path to implementation with familiar tools, this work aims to promote the wider adoption of timber flooring as a sustainable, eco-friendly, and aesthetically valuable technology.

5.1 Checking conventional timber-concrete composite floors and the proposed hybrid solution at equal floor thickness.

For varying floor thickness *H* and span length *L*, and disregarding the contribution of the steel profile, the performances of HybC floors as the one represented in **Fig. 11** are compared with those of corresponding TCC floors with same *L* and *H*, as the one represented in **Fig. 12**. The span lengths and cross-sectional configurations considered in this study were selected to represent the typical practical range of application of the proposed floor system. In particular, spans ranging from 5 to 7 m are representative of common building solutions for timber floors, and are therefore sufficient to assess the feasibility and structural performance of the proposed hybrid concept within its intended field of use. In particular, spans of 5 to 7 meters are representative of common timber floor solutions in building construction. According to the literature, such spans fall within the optimal range for this typology [56] The performed analysis is therefore sufficient to assess the feasibility and structural performance of the proposed hybrid concept within its intended field of application.

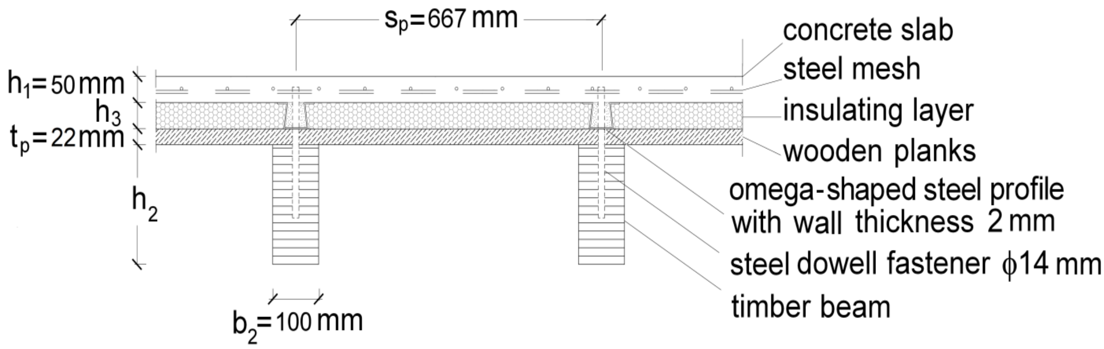

Fig. 11. Example of hybrid composite floor

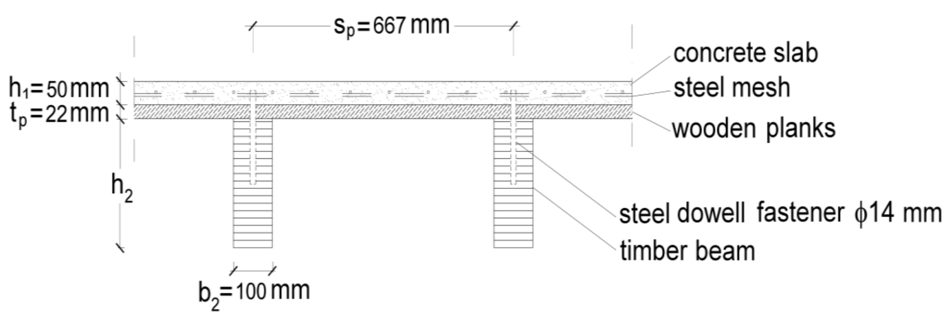

Fig. 12. Example of timber-concrete composite floor for performance comparison with the one of **Fig. 11**

Both floor types have same thickness of the concrete slab (h_1=50 mm) and wooden plank (t_a=22 mm), as well as same breadth (b_2=100 mm) and spacing (s_p=667 mm) of the timber beams (**Figs 11** and **12**).

Live loads of 2 kN/m^2 are assumed in both cases. With reference to the notation of the Eurocode 5 [10], the elastic modulus of timber is assumed to be E_2=$E_{0..mean}$=11600 MPa. Moreover, the bending, tensile and shear strengths of timber are $f_{m.g.k}$ = 24 MPa, $f_{t.0.g.k}$ =16.5 MPa, $f_{v.k}$ =2.7 MPa respectively.

A size factor k_h=$(600/h_2)^{0.1}$ is also applied (h_2 in mm) [10]),. Checking both HybC floor and TCC floor, k_{mod}=0.8 and 0.6 have been assumed for t = 0 and $t = \infty$, respectively, that is of course lower than k_{mod}=0.9 assumed for the timber-steel composite beams during the Con Ph. By referring to interior floors in buildings under controlled climate conditions (service class 1 [10]), k_{def} =0.6 has been assumed.

Also, for concrete strength class C25/30, with elastic modulus $E_{1.0}$=31500 MPa, creep coefficient ϕ=2 has been supposed.

The performances of both types of composite floors are compared for three floor depths (H=352, 362, 372 mm) and given L = 5 m, and for three span lengths (L = 5, 6, 7 m) and given H = 352 mm.

Since all HybC floors are chosen to have the same depth of the steel profile h_3=50 mm, then when the total depth of HybC floors is increased from H=352 mm to H=362 and 372 mm (for L increased from 5 m to 6, 7 m, respectively), the depth of the timber beams of HybC floors is consequently increased from h_2 = 230 mm to h_2 = 240 and 250 mm.

For TCC floor, the same floor depth increase is instead obtained through increasing the timber beams' depth from 280 mm (for L = 5 m) to 290 and 300 mm (for L = 6, 7 m, respectively), in order to compare HybC floors and TCC floors with same floor thickness H and span length L, for same thickness of the concrete slab and wooden plank.

5.1.1 Deflections

In **Fig. 13a**, deflections u of HybC floors and TCC floors with span length 5 m and floor thickness 352, 362 and 372 mm are compared. It can be observed that deflections of TCC floors and HybC floors are similar. Although the contribution of the steel profile is not taken into account, compliance of TCC floors and HybC floors is practically the same (even if a bit higher in TCC floors), that is their deflections differ on only 3.5% in the long-term, and even less (2%) in the short-term. **Fig. 13b** shows that, for different span lengths but same floor depth (H=352 mm), deflections u of HybC floors are very close to the corresponding ones of TCC floors with same H.

However, all HybC floors are stiff enough, with the maximum deflection/span ratio of 1/260 in the most critical case of L=7 m and H=352 mm.

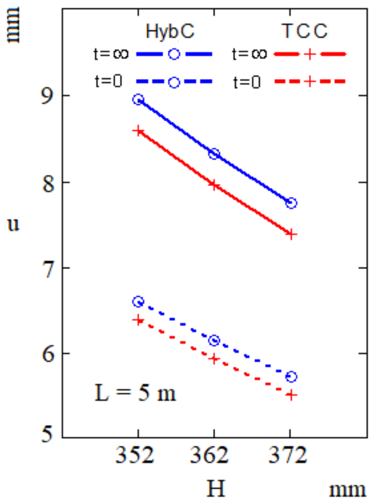

(a) For varying structural depth and given span length L = 5 m

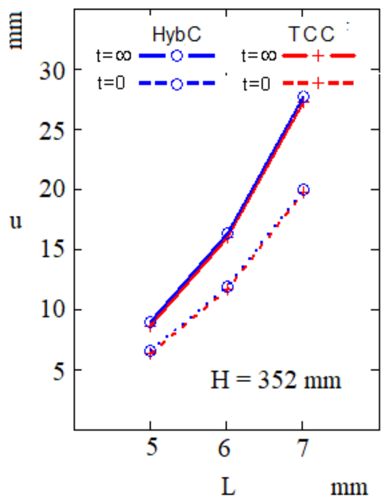

(b) For varying span length and given structural depth H=352 mm.

Fig. 13. Hybrid composite floor deflections.

5.1.2 Timber beams

Timber beams have been checked at the Ultimate Limit State by using the interaction formula (11) and considering different H and L. **Figs 14a** and **14b** show that, in terms of strength, timber beams of both HybC and TCC floors are highly affected by creep to the same extent.

In **Fig. 14a**, the results obtained checking both types of floors for L=5 m and H varying between 352 and 372 mm are compared. It can be seen that, in general, stress level in the timber beams of HybC and TCC floors is similar, but it is a bit higher in HybC floors than in TCC floors, since in the former case the depth of the timber beams is lower (h_2=230÷250 mm) than in the latter case (h_2=280÷300 mm).

Finally, checking at ultimate both types of floor with H=352 mm for span lengths varying between 5 and 7 m, timber beams of both HybC floors (h_2=230 mm) and TCC floor (h_2=280 mm) attain the Ultimate Limit State for L=6 m for long-term loads only (while not in the short-term).

For L= 7 m, the U.L.S. is instead practically attained also in the short term, but with $\sigma_{\infty}^{I\,(2)}$ much greater than 1 for long-term loading (**Fig. 14b**).

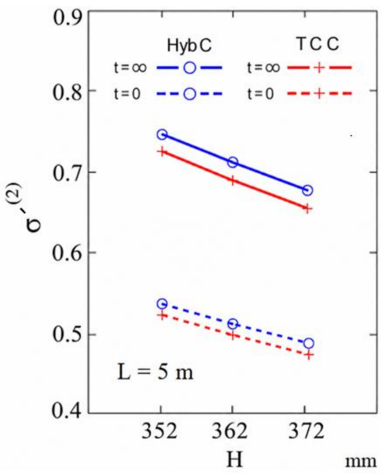

a) For varying structural depth and given span length L=5 m

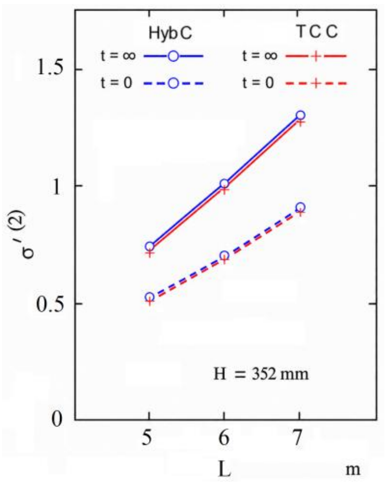

b) For varying span length and given structural depth H=352 mm

Fig.14. Verification of timber beams at the Ultimate Limit State subjected to combined axial force and bending.

Therefore, for L= 6 and 7 m, the HybC floors geometry must be updated. For HybC floors with L = 6 m, since the long-term ultimate stress in the timber beams is only little over the timber strength, the geometry needs to be only slightly modified to satisfy timber beams checks. This goal can be achieved if H is increased to 362 mm by increasing the depth of timber beams by 10 mm. Since moments vary with the square of span length, for L=7 m the depth increase must be higher to meet timber strength requirements. For instance, for h_3=50 mm, h_2 should be at least 290 mm, otherwise, using a thicker insulating layer, h_3 can be increased to 60 mm and h_2 can be reduced to 280 mm. Unfortunately, these latter solutions don't limit deflections sufficiently during the C Ph (see paragraph 3.4.1), thus needing deeper timber beams and/or deeper steel profiles. The latter, even if not taken into account in this simplified calculations of HybC floors, contribute to increasing the lever arm of the internal couple; the larger the lever arm, the greater the internal moment.

5.1.3 Concrete slab

Figs. 15a and **15b** show the results obtained by checking the top and bottom edges of the concrete slab of both types of floors at the U.L.S. for different floor thicknesses and span lengths.

In the short-term, tensile stresses at the bottom edge of TCC and HybC floors are very similar, and are both within the tensile strength of normal concrete currently used in timber composite floors, even more so if a steel reinforcement mesh is used, as usual. In the long-term, the tensile stresses at the slab intrados decrease significantly, and the slab can even become fully compressed, especially for higher bending moments occurring when L=7 m (see **Fig. 15b**)

Additionally, **Figs. 15a** and **15b** show that creep effects in the concrete slab of both types of floors tends to be higher, the higher is the stress level caused by lower floor depth for given L (**Fig. 15a**) and longer span length for given H (**Fig. 15b**). In the long-term, the decrease of both compressive and tensile stresses caused by creep effects is similar in both types of floors, although slightly higher in HybC than in TCC floor.

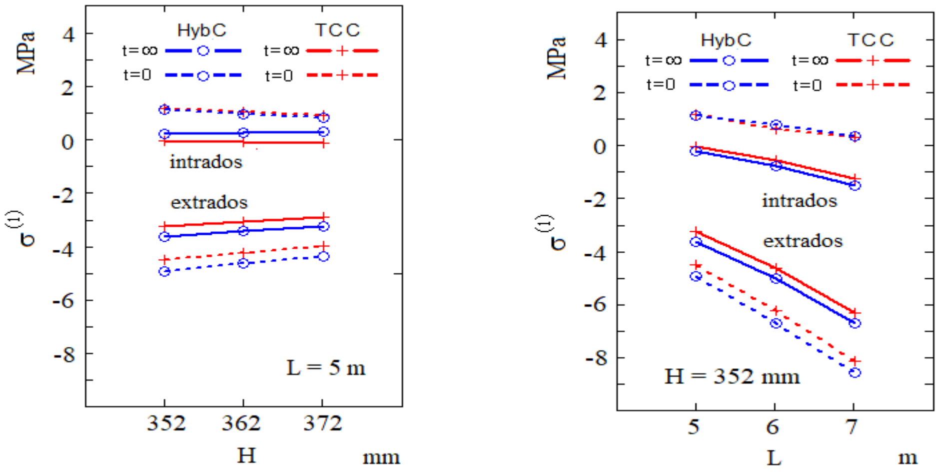

a) For varying structural depth and given span length L=5 m b) For varying span length and given structural depth H=352 mm.

Fig. 15. Verification of concrete slab at the Ultimate Limit State subjected to combined axial force and bending

5.1.4 Fastener

Both in the short- and in the long-term, both types of floors show to have similar results in terms of ultimate shear force F_d on the fastener. **Fig. 16a** and **16b** shows that F_d is always higher in the HybC than in the TCC floor with same H, differing of only a 10% in all the cases considered. Moreover, although timber and concrete have a time-dependent behaviour, long- and short-term values of F_d are practically the same both in HybC and in TCC floor [57].

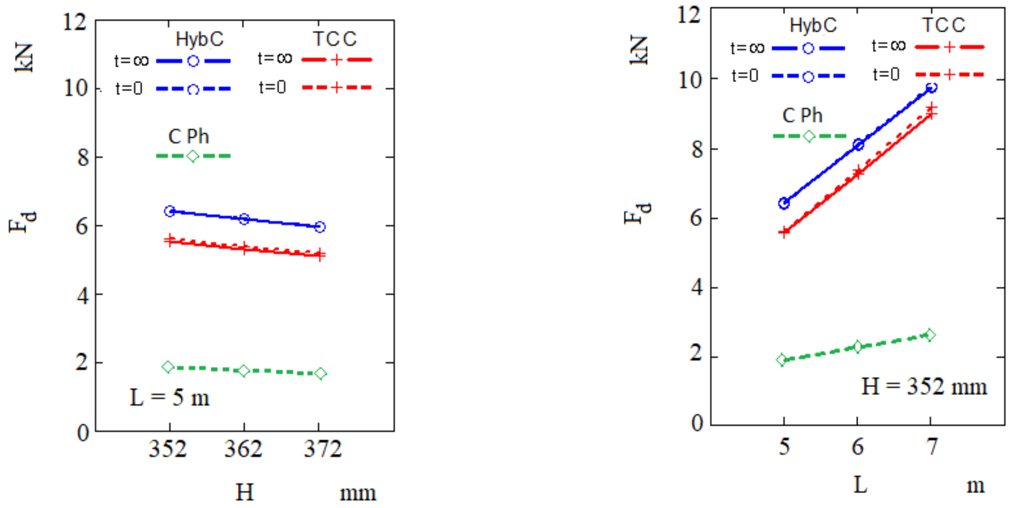

(a) For varying structural depth and given span length L=5 m (b For varying span length and given structural depth H=352 mm.

Fig.16. Design shear force on the fastener

Fig. 16a shows that by varying H for given L, that is by varying timber depth from 230 mm to 250 mm, the variation of the shear force on the fastener is rather low.

For given H, **Fig. 16b** instead shows that F_d increases with span length L, and for L=7 m and h_3=50 mm, almost attains the fastener resistance. Nevertheless, it is easy to either increase joint resistance R_d and/or decrease F_d. For instance, R_d can be increased by a 30% through only increasing the diameter of the fastener from 14 to 16 mm, while F_d can be decreased of a 10% by decreasing the equivalent spacing s_{eq} from 125 to 100 mm.

Finally, both **Figs. 16a** and **16b** clearly show that during the construction phase the design shear load on the fastener in the timber-steel composite beams (C Ph) is always much lower than in HybC floors.

6. Conclusions

Timber-concrete composite (TCC) floors are widely used in both new construction and renovation. This paper introduces a novel hybrid timber-steel-concrete composite floor designed to overcome key limitations of conventional TCC systems. The main mechanical advantage of the proposed system lies in the increased construction-stage stiffness provided by the timber–steel composite beam, which enables self-bearing behaviour during casting while preserving satisfactory structural performance after curing through simplified code-based design assumptions.

The primary innovation lies in a conceptual design that simplifies construction and streamlines structural calculation, thereby promoting the wider adoption of sustainable timber-based solutions.

The proposed hybrid system offers three primary advantages, as outlined below:

- Simplified Construction: The system eliminates the need for temporary propping during construction, as the integrated steel profile provides sufficient stiffness to support wet concrete and other construction loads. This reduces labor time and cost without increasing the final floor depth. Partial prefabrication in factory is also promoted. Furthermore, the system preserves the aesthetic appeal of exposed timber ceilings, a valued architectural feature. The adoption of the proposed construction technology can also be extended to renovation of historical buildings facilitating the retrofit of timber floors when higher load bearing capacity is required.

- Integrated Comfort and Efficiency: The design seamlessly accommodates acoustic and thermal insulation within the structural depth by positioning the insulating layer alongside the steel members. This is a critical advantage in multi-story buildings: in fact, since it does not require thicker floor thickness, it maximizes usable floor-to-ceiling height without compromising structural performance, a benefit highly valued by developers.

- Streamlined and Code-Compliant Design: The structural performance of the completed hybrid floor can be conservatively verified using established Eurocode 5 provisions.

Funding Statement

The research was funded by the University of Cagliari, Department of Civil & Environment Engineering, and Architecture.

CRediT authorship contribution statement

L. Fenu: Conceptualization, Methodology, Investigation, Formal analysis, Writing – original draft, Supervision. Editing **A. Aloisio**: Methodology, Investigation, Supervision, Writing – review & editing. **A. Hosseini**: Investigation, Review & editing. **G.F. Giaccu**: Methodology, Supervision**,** Review & editing. **B. Briseghella**: Methodology, Supervision**,** Review & editing.

Conflicts of Interest

The authors declare that they have no conflicts of interest to report regarding the present study.

Data Availability Statement

Some or all data, models, or codes that support the findings of this study are available from the corresponding author upon reasonable request.

References

[1] Ceccotti A. Composite structures. In: Thelanderson S, Larsen H, (Eds). Timber engineering. Chichester, UK, Wiley & Sons Inc 2003; 409–27.

[2] Piazza M, Turrini G. Advances in technology of joints for laminated timber. Analysis of the structural behaviour. In: Proceedings of the Working Commission CIB-W18-Timber Structures, Meeting 19,

International Council for Research and Innovation in Building and Construction, Florence 1986; CIB-W18/19-7-9.
[3] Piazza M, Tomasi R, Modena R. Elementi singoli composti. In: Strutture in legno. Milan, Hoepli (In Italian) 2005; 344–83.
[4] Yeoh D, Fragiacomo M, De Franceschi M, Boon KH. State of the art on timber-concrete composite structures: Literature Review. Journal of Structural Engineering, ASCE 2011; 137(10): 1085–1095. https://doi.org/10.1061/(ASCE)ST.1943-541X.0000353
[5] Dias A, Schänzlin J, Dietsch P. Design of timber-concrete composite structures. A state-of-the-art report. Auchen, Shaker Verlag 2018.
[6] Estévez-Cimadevila J, Martín-Gutiérrez E, Suárez-Riestra F, Otero-Chans D, Vázquez-Rodríguez JA. Timber-concrete composite structural flooring system. Journal of Building Engineering 2022; 49: 104078. https://doi.org/10.1016/j.jobe.2022.104078.
[7] Pastori S, Mazzucchelli ES, Wallhagen M. Hybrid timber-based structures: A state of the art review. Construction and Building Materials 2022; 359: 129505. https://doi.org/10.1016/j.conbuildmat 2022.129505.
[8] Tsalkatidis T, Alhussain MM. Numerical study of a hybrid timber–concrete floor system. In: In: Kioumarsi, M., Shafei, B. (Eds) The 1st International Conference on Net-Zero Built Environment. NTZR 2024. Lecture Notes in Civil Engineering, vol 237. Springer, Cham 2025; 1371-1380. https://doi.org/10.1007/978-3-031-69626-8_115.
[9] Quang Mai K, Park A, Nguyen KT, Lee K. Full-scale static and dynamic experiments of hybrid CLT–concrete composite floor. Construction and Building Materials 2018; 170 (2): 55–65. https://doi.org/10.1016/j.conbuildmat.2018.03.042.
[10] EN 1995-1-1. Eurocode 5: Design of timber structures Part 1-1: General, Common rules and rules for buildings. European Committee for Standardization. CEN, Brussels, Belgium 2004.
[11] Ceccotti A. Composite concrete-timber structures. Progress in Structural Engineering and Materials 2002; 1; 4(3): 264–275. https://doi.org/10.1002/pse.126.
[12] Möhler, K. Über das Tragverhalten von Biegeträgern und Druckstäben mit zusammengesetzten Querschnitt und nachgiebigen Verbindungsmitteln. Ph.D. Thesis, Karlsruhe Institute of Technology, Karlsruhe, Germany 1956. https://publikationen.bibliothek.kit.edu/1000172658.
[13] Newmark N, Siess C, Viest I. Tests and analysis of composite beams with incomplete interaction. Proceedings, Society for Experimental Stress Analysis 1951; 9(1): 75–92.
[14] Ceccotti A, Fragiacomo M, Giordano S. Long-term and collapse tests on a timber-concrete composite beam with glued-in connection. Materials and Structures 2007; 40(1): 15–25. https://doi.org/10.1617/s11527-006-9094-z.
[15] Yeoh D, Fragiacomo M, Aldi P, Mazzilli M, Kuhlmann U. Performance of notched coach screw connection for timber-concrete composite floor system. In: Proceedings of the 10-th World Conference on Timber Engineering (WCTE). Miyazaki, Japan 2008; 294-301.
[16] Kavaliauskas S, Kvedaras A, B. Valiūnas. Mechanical behaviour of timber-to-concrete connections with inclined screws. Journal of Civil Engineering and Management 2007; 13(3): 193–199. https://doi.org/10.3846/13923730.2007.9636437.
[17] Symons D, Persaud R, Stanislaus H. Slip modulus of inclined screws in timber-concrete floors. Proceedings of the Institution of Civil Engineers: Structures and Buildings 2010; 163(4): 245–55. https://doi.org/10.1680/stbu.2010.163.4.245.
[18] Du H, Hu X, Xie Z, Wang H. Study on shear behavior of inclined cross lag screws for glulam-concrete composite beams. Construction and Building Materials 2019; 224: 132–43. https://doi.org/10.1016/j.conbuildmat.2019.07.035.
[19] Di Nino S, Gregori A, Fragiacomo M. Experimental and numerical investigations on timber-concrete connections with inclined screws. Engineering Structures 2020; 209: 109993. https://doi.org/10.1016/j.engstruct.2019.109993.
[20] Cao J, Xiong H, Chen J. Mechanical performance of timber-concrete bolted connections under cyclic loading. Structures 2021; 34: 3464–3477. https://doi.org/10.1016/j.istruc.2021.09.086.
[21] Martín-Gutiérrez E, Estévez-Cimadevila J, Otero-Chans D, Suárez-Riestra F. Discontinuous π-form steel shear connectors in timber-concrete composites. An experimental approach. Engineering Structures 2020; 216: 110719. https://doi.org/10.1016/j.engstruct.2020.110719.
[22] Kuhlmann U, Michelfelder B. Grooves as shear-connectors in timber-concrete composite structures. In: Proceedings of the 8-th World Conference on Timber Engineering (WCTE). Lahti, Finland 2004; 301–306.
[23] Balogh J, Gutkowski R, Wieligmann M, Haller P. Mechanics behavior of dowel connections for partially composite wood-concrete beams. In: Proceedings of the 7-th World Conference on Timber Engineering (WCTE). Shah Alam, Malaysia 2002; 290–295.
[24] Gutkowski RM, Brown K, Shigidi A, Natterer J. Investigation of notched composite wood–concrete connections. Journal of Structural Engineering 2004; 130(10): 1553–1561. https://doi.org/10.1061/(ASCE)0

733-9445(2004)130:10(1553)
[25] Zhang L, Zhou J, Chui YH. Development of high-performance timber-concrete composite floors with reinforced notched connections. Structures 2022; 39: 945–57. https://doi.org/10.1016/j.istruc.2022.03.074
[26] Fragiacomo M, Gutkowski R, Balogh J, Fast R. Long-term behaviour of wood-concrete composite beams with notched connection detail. In: Proceedings of the 9th World Conference on Timber Engineering (WCTE). Portland, Oregon, USA 2006; 1(19): 3, 8.
[27] Lukaszewska E, Johnsson H, Fragiacomo M. Performance of connections for prefabricated timber–concrete composite floors. Materials and Structures 2008; 41(9): 1533–1550. https://doi.org/10.1617/s11527-007-9346-6.
[28] Piazza M, Ballerini M. Experimental and numerical results on timber-concrete composite floors with different connection systems. In: Proceedings of the 6-th World Conference on Timber Engineering (WCTE). Whistler Resort, British Columbia, Canada 2000; CD.
[29] Rasmussen PK, Sørensen JH, Hoang LC, Feddersen B, Larsen F. Notched connection in timber-concrete composite deck structures: A literature review on push-off experiments & design approaches. Construction and Building Materials 2023; 397: 131761. https://doi.org/10.1016/j.conbuildmat.2023.131761.
[30] Jurkiewiez B, Durif S, Bouchair A, Grazide C. Experimental and analytical study of hybrid steel-timber beams in bending. Structures 2022; 39: 1231–1248. https://doi.org/10.1016/j.istruc.2022.03.055.
[31] Chybiński M, Polus Ł. Experimental and numerical investigations of aluminium-timber composite beams with bolted connections. Structures 2021; 34: 1942–1960. https://doi.org/10.1016/j.istruc.2021.08.111.
[32] Gilbert BP, Guan H, Ngo T, Remennikov A. Shear performance of glued and screwed timber-steel composite connections for composite timber-steel beams. Construction and Building Materials 2024; 450: 138762. https://doi.org/10.1016/j.conbuildmat.2024.138762.
[33] Chen, Z., Dagenais, C., Tung, D., Wu, T., Gaglione, M.. Fire testing and modeling of a novel hybrid timber floor system. Journal of Structural Engineering 2025; 151(1): 4024186. https://doi.org/10.1061/JSENDH.STENG-13554.
[34] Owolabi D, Loss C. Experimental and numerical study on the bending response of a prefabricated composite CLT-steel floor module. Engineering Structures 2022; 260: 114278. https://doi.org/10.1016/j.engstruct.2022.114278.
[35] Aloisio A, Pasca DP, Owolabi D, Loss C. Vibration serviceability of hybrid CLT-steel composite floors based on experimental and numerical investigations using random walk models. Engineering Structures 2024; 304: 117600. https://doi.org/-10.1016/j.engstruct.2024.117600.
[36] Owolabi D, Aloisio A, Loss C. Vibration attenuation in cross-laminated timber–steel composite floors using loose sand as a passive damping mechanism. Engineering Structures 2025; 340: 120642. https://doi.org/10.1016/j.engstruct.2025.120642.
[37] Gelfi P, Giuriani E, Marini A. Stud shear connection design for composite concrete slab and wood beams. Journal of Structural Engineering 2002; 128(12): 1544–1550. https://doi.org/10.1061/(ASCE)0733-9445(2002)128:12(1544)
[38] Gelfi P, Giuriani E. Influence of slab-beam slip on the deflection of composite beams. International Journal for Restoration of Buildings and Monuments 2003; 9(5): 475–490.
[39] Djoubissié Denouwé D, Messan A, Fournely E, Bouchair A. Influence of interlayer in timber-concrete composite structures with threaded rebar as shear connector-experimental study. American Journal of Civil Engineering and Architecture 2018; 6(1): 38–45. https://doi.org/10.12691/ajcea-6-1-5.
[40] Carvalho JLF, Rodrigues LSM, Pires CHM. Interlayer influence on timber-lwac composite structures with screw connections. Journal of Structural Engineering 2011; 137(5): 618–24. https://doi.org/10.1061/(ASCE)ST.1943-541X.0000299
[41] Gutkowski RM, Balogh J, To LG. Finite-element modeling of short-term field response of composite wood-concrete floors/decks. Journal of Structural Engineering 2010; 136(6): 707–714. https://doi.org/10.1061/(ASCE)ST.1943-541X.0000117
[42] EN 1992-1-1. Eurocode 2 : Design of concrete structures Part 1-1: Genera rules and rules for buildings. European Committee for Standardization. CEN, Brussels, Belgium 2004.
[43] EN 1993-1-1. Eurocode 3 : Design of steel structures Part 1-1: Genera rules and rules for buildings. European Committee for Standardization. CEN, Brussels, Belgium 2005.
[44] Gelfi P, Giuriani E. Studio sperimentale del comportamento di travi miste legno-acciaio con connettori a piolo. (In Italian). In: Scibilia N (Ed). Strutture composte. Proceedings of the 4th Italian Workshop on composite structures. Palermo, Italy 2000; 254–268.
[45] Kreutzinger H. Mechanically jointed beams and columns. In: Timber Engineering 1. Centrum Hout, Almere, The Netherlands 1994; B11/1–B11/10.
[46] DIN - 1052 | 2008 - 12. Entwurf, Berechnung und Bemessung von Holzbauwerken. Allgemeine Bemessungsregeln und Bemessungsregeln für den Hochbau. Allgemeine Bemessungsregeln und Bemessungsregeln für den Hochbau 2008.

[47] EN 1993-1-8. Eurocode 3: Design of steel structures part 1.8: Design of joints. European Committee for Standardization. CEN, Brussels, Belgium 2007.
[48] Fenu L, Bozano E. Solaio composito parzialmente prefabbricato con soletta in calcestruzzo e travi in legno connesse a profilati in acciaio. In: Proceedings of the 22-nd CTA Congress - L'acciaio per un futuro sostenibile (In Italian). Padua, Italy 2009; 493–504.
[49] Tsai SW, Hahn HT. Strength of composite materials. In. Introduction to composite materials. Technomic Publisher, Westport, Connecticut 1980; 277-329.
[50] Toscano S. Solai composti con tre membrature, Legno-Acciaio-Calcestruzzo. Sperimentazione (In Italian). Master Thesis. Università di Cagliari, Italy 2017.
[51] Hoffmeyer P. Strength under long-term loading. In: Thelanderson S, Larsen H, (Eds). Timber engineering. Chichester, UK, Wiley & Sons Inc 2003; 131–152.
[52] Mårtensson A. Short- and long-term deformations in timber structures. In: Thelanderson S, Larsen H, (Eds). Timber engineering. Chichester, UK, Wiley & Sons Inc 2003; 221–240.
[53] Fragiacomo M, Ceccotti A. Long-term behavior of timber–concrete composite beams. I: Finite element modeling and validation. Journal of Structural Engineering 2006; 132(1): 13–22. https://doi.org/10.1061/(ASCE)0733-9445(2006)132:1(13)
[54] Fragiacomo M. Long-term behavior of timber–concrete composite beams. ii: numerical analysis and simplified evaluation. Journal of Structural Engineering 2006; 132(1): 23–33. https://doi.org/10.1061/(ASCE)0733-9445(2006)132:1(23)
[55] Johansen, KW. Theory of timber connections. International Association of Bridge and Structural Engineering 1949; 9: 249–262. https://www.e-periodica.ch/digbib/view?-lang=en&pid=bse-me-001%3A1949%3A9%3A%3A292.
[56] Jelusic P, Kravanja S. Optimal design of timber-concrete composite floors based on the multi-parametric MINLP optimization. Composite Structures 2017; 179: 285–93. https://doi.org/10.1016/j.compstruct.2017.07.062.
[57] Amadio C., Ceccotti A., Di Marco R., Fragiacomo M. Numerical evaluation of long-term behaviour of timber-concrete composite beams. In: Proceedings of the 6-th World Conference on Timber Engineering (WCTE). Whistler Resort, British Columbia, Canada 2000; CD-ROM: 9.